Future Integrative Medicine **2025** vol. 4(2) | 88–101
DOI: 10.14218/FIM.2025.00003

Original Article

Protective Effects of Ejiao on Chronic Obstructive Pulmonary Disease in Mice via Modulation of the ER/AKT/NF-κB Pathway

Siman Sun[1,2#], Tianyu Zhou[1,2#], Xiaoyu Fan[2#], Haiyan Jiang[2], Jie Li[2], Zeao Xu[3], Wanfang Li[2,4], Xiangfeng Ye[4], Chuan Wang[1], Fuwei Xie[5], Pingping Shang[5], Bin Wang[1*] and Hongtao Jin[2,4,6*]

[1]College of Pharmacy, Shaanxi University of Chinese Medicine, Xianyang, Shaanxi, China; [2]New Drug Safety Evaluation Center, Institute of Materia Medica, Chinese Academy of Medical Sciences and Peking Union Medical College, Beijing, China; [3]College of Life Sciences and Biopharmaceuticals, Shenyang Pharmaceutical University, Shenyang, Liaoning, China; [4]Beijing Union-Genius Pharmaceutical Technology Development Co., Ltd., Beijing, China; [5]Zhengzhou Tobacco Research Institute of CNTC, Zhengzhou, Henan, China; [6]NMPA Key Laboratory for Safety Research and Evaluation of Innovative Drug, Beijing, China

Received: January 07, 2025 | **Revised:** March 01, 2025 | **Accepted:** March 21, 2025 | **Published online:** April 16, 2025

Abstract

Background and objectives: Chronic obstructive pulmonary disease (COPD) is an irreversible inflammatory lung disease. Studies have shown that macrophages and estrogen receptors play a pivotal regulatory role in the development of COPD. Ejiao (*Colla Corii Asini*, CCA, or donkey-hide gelatin), a traditional Chinese medicine, has anti-inflammatory and lung function-protective effects, but its specific mechanism in COPD remains unclear. This study aimed to explore the immunomodulatory effects of Ejiao on COPD, focusing on its impact on inflammatory pathways and macrophages.

Methods: This study is the first to apply a network pharmacology approach to explore the potential mechanisms underlying Ejiao's therapeutic effects on COPD. We collected the peptides and chemical components of Ejiao and used the STRING database to screen for COPD-related targets of Ejiao components, constructing a drug-molecular network. Additionally, we established cigarette smoke extract (CSE) and lipopolysaccharide-induced cell injury models and treated them with Ejiao-containing serum. Western blot (WB) analysis was used to detect the expression of related proteins, enabling a preliminary exploration of Ejiao's effects and regulatory mechanisms. In further experiments, a mouse COPD model was established, and eight weeks of Ejiao intervention were conducted. We assessed lung function, pathological changes in lung tissue, monitored cytokine levels in serum and bronchoalveolar lavage fluid, performed flow cytometry to evaluate abdominal macrophage levels, and conducted WB to analyze protein expression, providing an in-depth study of Ejiao's regulatory effects on the mouse COPD model.

Results: The findings from the network pharmacology analysis suggest a potential regulatory role of the estrogen receptor pathway in COPD. CSE stimulation of RAW264.7 cells resulted in elevated tumor necrosis factor-α levels, decreased interleukin-10 levels, reduced expression of estrogen receptors (ERs) α and β, decreased inhibitor of NF-κB levels, and increased p-AKT levels. Following Ejiao intervention, interleukin-10, ERα+β, and inhibitor of NF-κB levels increased, while p-AKT levels decreased. Ejiao significantly improved lung function in CSE/lipopolysaccharide-induced COPD mice, reduced the number of macrophages, lowered the levels of inflammatory factors in bronchoalveolar lavage fluid, and increased estradiol levels in serum. WB results indicated that Ejiao may ameliorate lung injury in COPD by modulating the ER/AKT/NF-κB pathway.

Conclusions: The results suggest that Ejiao may improve lung injury and inflammation in CSE/ lipopolysaccharide-induced COPD by regulating the ER/AKT/NF-κB pathway.

Keywords: Chronic obstructive pulmonary disease; Estrogen receptors; Ejiao; Network pharmacology; AKT; NF-κB.

[*]**Correspondence to:** Bin Wang, College of Pharmacy, Shaanxi University of Chinese Medicine, Xianyang, Shaanxi 712000, China. ORCID: https://orcid.org/0000-0002-8305-8667. Tel: +86-13892981087; E-mail: wangbin@sntcm.edu.cn; Hongtao Jin, New Drug Safety Evaluation Center, Institute of Materia Medica, Chinese Academy of Medical Sciences and Peking Union Medical College, Beijing 100000, China. ORCID: https://orcid.org/0000-0002-0638-707X. Tel: +86-13911262199; E-mail: jinhongtao@imm.ac.cn

[#]Contributed equally to this work.

How to cite this article: Sun S, Zhou T, Fan X, Jiang H, Li J, Xu Z, *et al*. Protective Effects of Ejiao on Chronic Obstructive Pulmonary Disease in Mice via Modulation of the ER/AKT/NF-κB Pathway. *Future Integr Med* 2025;4(2):88–101. doi: 10.14218/FIM.2025.00003.

Introduction

Chronic obstructive pulmonary disease (COPD) is a chronic inflammatory lung disease characterized by persistent airflow limitation, often associated with factors such as smoking history and environmental pollution.[1] Research has demonstrated that smoking triggers an inflammatory response in the airways, primarily through the activation of macrophages and other immune cells.[2] The accumulation of macrophages in the lungs releases inflammatory mediators, such as tumor necrosis factor-α (TNF-α) and interleukin (IL)-8, which promote the inflammatory process that exacerbates COPD.[3–5] Studies have shown that the NF-κB signaling pathway plays a crucial role in the pathogenesis of COPD.[6] AKT (protein kinase B), the central component of the PI3K/AKT signaling pathway,[7,8] can directly phosphorylate the IκB kinase complex, promote the degradation of IκB, and thus activate NF-κB. Furthermore, studies suggest that female reproductive factors may contribute to the development of COPD by modulating the hormonal milieu in women.[9] Estrogen (E2) exhibits a wide array of biological effects in women, including antioxidant and anti-inflammatory properties, which may play a role in alleviating lung injury.[10] The level of E2 in women gradually decreases, which may lead to increased sensitivity of the lungs to harmful substances (such as tobacco smoke), thereby increasing the risk of COPD. Studies have shown that E2 can regulate the production of inflammatory mediators and cytokine expression by macrophages through estrogen receptors (ERs), reducing the production of pro-inflammatory cytokines.[11] ERs are divided into two types, ERα and ERβ, which regulate the transcription of specific genes in the cell nucleus by binding to estrogen.[12] The interaction between ER and AKT signaling pathways mainly occurs during cell signaling. ER can be activated in an estrogen-dependent or -independent manner, involving signaling through PI3K and AKT.[13] In summary, ER may modulate the inflammatory response in COPD by regulating upstream signaling molecules of the NF-κB pathway and influencing NF-κB activity. The AKT/NF-κB signaling pathway plays a crucial role in cell survival and proliferation. Investigating the interplay between estrogen and the AKT/NF-κB signaling pathway could offer new insights into the pathogenesis of COPD and pave the way for innovative therapeutic strategies.

Ejiao (*Colla Corii Asini*, CCA, or donkey-hide gelatin) is a traditional Chinese medicine with a rich history spanning over 2,000 years. Ejiao is a solid gelatin block derived from donkey skin through a meticulous process of decoction and concentration. Its primary components include collagen, amino acids, dermatan sulfate, and trace elements.[14] Renowned for its diverse pharmacological properties, Ejiao has been shown to promote hematopoiesis, nourish yin, moisturize the lungs, enhance immunity, and exhibit anti-infection, anti-aging, anti-tumor, and anti-fatigue effects.[15] Moreover, it is considered relatively safe for use.[16] A study found that Ejiao may have a positive effect on inhibiting the dominant response of Th2 cells in asthma, helping to regulate the balance of Th1/Th2 cytokines and reduce eosinophilic inflammation in the lungs of asthmatic rats. It also reduced the infiltration of inflammatory cells in the lungs of rats to some extent.[17] Yue *et al*.[18] established an acute lung injury model by instilling lipopolysaccharide (LPS) into the nasal cavity of C57BL/6N mice and found that Ejiao could play an anti-inflammatory role in acute lung injury by reducing the expression of NF-κB pathway proteins and their downstream proteins related to cell pyroptosis, as well as reducing the production of mitochondrial reactive oxygen species in inflammatory lung cells. In addition, one study has shown that Ejiao can improve respiratory function impairment caused by inhalation of artificial fine particles in rats, inhibiting the abnormal proliferation of lung macrophages and showing a protective effect on lung function.[19] Furthermore, a study has shown that Ejiao may protect rats from lung injury caused by intratracheal instillation of fine particles by inhibiting the excessive proliferation of pulmonary macrophages, reducing malondialdehyde content, and increasing glutathione peroxidase activity.[20] Macrophages are the first line of defense for the body and clear infections by engulfing and killing pathogenic microorganisms.[21] However, the specific mechanism by which Ejiao regulates macrophages to protect lung function remains unclear. Therefore, this study aimed to systematically analyze the interaction network between the active ingredients in donkey-hide gelatin and COPD-related targets by integrating *in vivo* and *in vitro* experiments and combining network pharmacology database analysis. Additionally, this study seeks to explore the potential lung-protective mechanism of donkey-hide gelatin in COPD, which can improve research efficiency and provide data support for further investigations.

Materials and methods

Network pharmacology

The main components of Ejiao were identified through an extensive search in HERB, SymMap, PubMed, Sino Med, and CNKI. The structures of these compounds were constructed and visualized using ChemDraw 20.0 and Chem3D 20.0 software. Target networks were constructed based on the identified compounds, amino acids, and small molecule peptides.[22] The canonical simplified molecular input line entry system (SMILES) representations of the compounds were collected from the PubChem database for further analysis. After obtaining the SMILES representations, the SwissTargetPrediction website was utilized to predict the potential targets of the main components of Ejiao. By integrating the target data for the compounds, amino acids, and peptides present in Ejiao, a comprehensive list of relevant targets was compiled for further analysis. To collect disease targets related to COPD, we used "Chronic obstructive pulmonary disease" as the keyword in the GeneCards (https://www.genecards.org/), OMIM (https://www.omim.org/), and DrugBank (https://go.drugbank.com/) databases. The median of the disease targets for COPD in GeneCards was taken according to the "Relevance score," duplicates were removed, and important target information was obtained. After integration, duplicate values were removed to obtain the corresponding targets for COPD disease.[23] In the STRING platform, the "Multiple proteins" module was selected, the intersection targets were entered, "Homo sapiens" was chosen as the source, and the "SEARCH" button was clicked. The minimum confidence level was set to 0.400, and proteins with non-interacting relationships were removed to generate a protein-protein interaction network diagram. The obtained TSV format files were imported into Cytoscape 3.7.1 software for network topology analysis, highlighting targets with strong associations. Gene Ontology (GO) functional enrichment analysis and Kyoto Encyclopedia of Genes and Genomes (KEGG) pathway enrichment analysis were performed on the intersection targets using the DAVID (https://david.ncifcrf.gov/) database. The drug-disease targets were placed into the DAVID database, with OFFICIAL-GENE-SYMBOL selected for Identifier, Homo sapiens for Species, and Gene List selected for submission. The results were sorted by Count value, and the top 10 GO-enriched biological process (BP), cellular component (CC), and molecular function (MF) results, along with the top 20 KEGG-enriched results, were

selected. The enrichment analysis results for the GO project's BP, CC, MF, and KEGG pathway were visualized using the Microbial Informatics Platform (http://www.bioinformatics.com.cn/).[24]

RAW264.7 cell culture

Mouse RAW264.7 macrophages were obtained from the Shanghai Cell Bank and maintained in an incubator at 37°C under a 5% CO_2 atmosphere. Dulbecco's modified eagle medium (DMEM) complete medium (VivaCell, C3130-0500, China) was used for culture, and the medium was supplemented with 15% fetal bovine serum (VivaCell, C04001, China) and 1% penicillin-streptomycin (Applygen, B3034, China).

Cell viability test

RAW264.7 cells in the logarithmic growth phase were seeded into 96-well plates at a density of 5×10^4 cells/mL, with 200 μL per well. The 96-well plates were then incubated at 37°C with 5% CO_2 overnight to allow the cells to adhere to the surface and proliferate. Different concentrations of CSE (provided by Zhengzhou Tobacco Research Institute, China), ranging from 0 to 200 μg/mL (0, 2.5, 5, 10, 20, 40, 80, 160, 200 μg/mL), were applied to treat the cells. After 12 and 24 h, cell counting kit-8 (CCK8) reagent (LABLEAD, CK001, China) was added according to the kit instructions. After a 2-h incubation, cell viability was assessed by measuring absorbance at 450 nm using an enzyme-linked immunosorbent assay (ELISA) reader to calculate the cell viability of each group.

Preparation of Ejiao-containing serum and cell viability test

Seven specific pathogen-free male Sprague-Dawley rats (six to eight weeks old) were purchased from Beijing Weitong Lihua Experimental Animal Technology Co., Ltd. and randomly divided into a control group of three rats and a drug-containing serum preparation group of four rats. The control group received normal saline via gavage, while the drug-containing serum preparation group was administered 4 g/kg of Ejiao solution (Shandong Dong'e Ejiao Co., Ltd., China) twice daily for three consecutive days. The Ejiao used in our experiment was commercially available Ejiao powder donated by Shandong Dong'e Ejiao Co., Ltd. It was stored at room temperature and prepared into a suspension with 0.1% sodium carboxymethyl cellulose before use. On the third day, one hour after the final administration, the rats were anesthetized, and blood samples were collected from the abdominal aorta. The blood was stored at 4°C overnight, and serum was separated by centrifugation at 3,000 rpm for 10 m. The serum was then heat-inactivated in a water bath at 56°C for 30 m, followed by filtration, aliquoting, and storage at −80°C for future use. RAW264.7 cells in the logarithmic growth phase were plated into 96-well plates at a density of 5×10^4 cells/mL, with 200 μL added to each well, and incubated overnight. The cells were then treated with 0–15% Ejiao-containing serum for 24 h. Following treatment, CCK8 reagent was added as per the kit instructions. After a 2-h incubation, absorbance at 450 nm was measured using an ELISA reader to evaluate cell viability in each group. These results were used to determine the optimal drug concentration for subsequent cell experiments.

Cell experiments

RAW264.7 cells were divided into five treatment groups: control group, CSE group, CSE + 5% Ejiao medicated serum group, CSE + 10% Ejiao medicated serum group, and CSE + 15% Ejiao medicated serum group. The cells were seeded into six-well plates at a density of 5×10^4 cells/mL per well and incubated at 37°C with 5% CO_2 for 12 h. After incubation, the cells from each group were collected for subsequent Western blot analysis to assess differences in protein expression among the groups.

Establishment and grouping of COPD animal model

This experiment utilized 70 specific pathogen-free female C57BL/6N mice, weighing 18–22 g, obtained from Beijing Weitonglihua Laboratory Animal Technology Co., Ltd. The animal experiment was approved by the Animal Ethics Committee of Beijing Union Jianhao Pharmaceutical Technology Development Co., Ltd., under the ethics approval number PDE-2301.

The mice were randomly divided into seven groups: the control group, solvent control group, model group, low-dose Ejiao group (2 g/kg), medium-dose Ejiao group (4 g/kg), high-dose Ejiao group (8 g/kg), and the Roflumilast group (P, 1 mg/kg; Livning, R126602-1G, China). The control group received 1 mL/kg phosphate-buffered saline (PBS) (Livning, LVN10022) solution via intranasal instillation, while the solvent control group was administered 1 mL/kg dimethyl sulfoxide (DMSO) solution (0.1 mg/mL) intranasally. Additionally, 10 mL/kg CMC-Na (0.1%) solution was gavaged six times a week. The remaining groups received 1 mL/kg CSE (0.1 mg/mL) solution intranasally five times a week, 1 mL/kg LPS (1 mg/mL) solution once a week, and the corresponding drugs were gavaged for eight weeks. After eight weeks, lung tissues and bronchoalveolar lavage fluid (BALF) were collected for subsequent analysis.

Respiratory function test

The EMKA WBP whole-body plethysmography system (EMKA, France) was used to measure the lung function data of mice. The mice were placed in a plethysmography chamber of the lung function test device. Prior to testing, the mice were allowed to acclimate to the environment for 5–10 m. Subsequently, key lung function parameters were monitored every 10–20 m. Changes in lung function were recorded and analyzed on days 15, 27, 31, 35, 39, and 42 of the study.

After intraperitoneal injection of sodium pentobarbital at 90 mg/kg for complete anesthesia, the trachea was exposed, and a tracheal tube was inserted and secured with sutures. The tracheal tube was connected to the FlexiVent forced oscillation small animal pulmonary function test device (EMKA, France) to monitor the main indicators of pulmonary function.

Hematology and blood biochemistry tests

After the forced oscillation lung function test, pre-cooled PBS lavage fluid was slowly injected into the alveoli through the endotracheal tube. After a brief interval, the fluid was carefully withdrawn and centrifuged to separate the cellular components and the supernatant. Centrifugation was conducted at 2–8°C, 3,000 rpm for 20 m. The supernatant was then carefully removed and transferred to a sterile centrifuge tube, while the precipitate was retained for analysis of the cell components in the BALF. Next, the lower end of the mouse sternum was pressed to find the apex beat, and a 1 mL syringe was used to vertically pierce the apex, slowly withdraw blood, and transfer it to a 1.5 mL centrifuge tube to avoid bubbles. After standing for 30 m to 1 h, the sample was centrifuged at 3,500 rpm for 15 m at 4°C, and the supernatant was aliquoted.

Histological evaluation and pathological scoring criteria

Lung tissues were preserved in a 4% paraformaldehyde buffer for 24–72 h, subjected to alcohol gradient dehydration, immersed in paraffin for embedding, and subsequently sliced into 4 μm sections and stained with hematoxylin-eosin for histomorphological evalu-

ation. Histological sections were observed using an optical microscope (Olympus, Japan). Five fields of view (×200 magnification) were randomly selected for each sample, and semi-quantitative scores of 0–4 were assigned for the above four indicators (semi-quantitative assessment index, IQA). The sum of the scores from the five fields of view for each animal was calculated to determine the average score for the group.

ELISA

ELISA (Elabscience, China) was employed to measure the concentrations of TGF-β, IL-10, IL-1β, and COX-2 in BALF, while E2 levels in mouse serum were determined following the instructions provided by the respective assay kits.

Flow cytometry

Five milliliters of pre-cooled PBS was slowly injected into the mouse peritoneal cavity to collect peritoneal macrophages. The accumulated fluid was then extracted, centrifuged, and resuspended for cell count analysis. After 12–18 h of culture, the cells were harvested and divided into experimental groups: negative/blank control, single staining/positive control, isotype control, fluorescence minus one control, biological control, and experimental group. A 100 µL aliquot of the cell suspension was added to each tube. To minimize nonspecific binding, 1 µg/100 µL of CD16/32 (Elabscience, China) was added to each tube and incubated at room temperature for 15 m. According to the experimental design, except for the blank control, 5 µL of each antibody, including fluorescein isothiocyanate (FITC)-labeled CD11b (Elabscience, E-AB-F1081C), PerCP/Cyanine5.5-labeled F4/80 (Elabscience, E-AB-F0995J), and PE-labeled CD86 (Elabscience), was added to the sample tubes. The samples were then incubated at 4°C in the dark for 30 m. Before flow cytometry analysis, 1 mL of cell staining buffer (Elabscience, E-CK-A107) was added to each sample, followed by centrifugation at 300g for 5 m. The supernatant was carefully discarded, and the cell pellet was resuspended in 200 µL of fresh cell staining buffer. Instrument parameters were adjusted to detect CD86+ CD11b+ F4/80+ macrophages.

Western blot

Homogenized lung tissue and treated RAW264.7 cells were lysed in RIPA lysis buffer (Lablead, R1091) at 4°C for 10 m, followed by centrifugation at 12,000 rpm for 15 m at 4°C. The protein content in the supernatant was quantified using the BCA protein assay kit (Lablead, B5001). Equal protein samples were separated on a gradient SDS-PAGE (Beyotime, P0688, China) and transferred to polyvinylidene difluoride membranes (LABLEAD, ISEQ00010-1), blocked with 5% BSA (Solarbio, A8010, China) at room temperature for 2 h, and then incubated with corresponding primary antibodies (Cell Signaling Technology, USA) at 4°C overnight. After washing the membranes with Tris-Buffered Saline with Tween® 20 (TBST) (TBS (LABLEAD, T7210M/B) containing 0.1% Tween-20 (Biotopped, T6220, China)), they were incubated with secondary antibodies (Cell Signaling Technology, #7074) for 2 h. Immunoreactive protein bands were detected using enhanced chemiluminescence (ECL, Tanon, 180-501, China).

Statistical analysis

The data are presented as mean ± standard deviation (Mean ± SD). One-way analysis of variance was employed to assess the differences between groups. In cases where the assumption of homogeneity of variances was met, the LSD test was used; otherwise, the Tamhani test was applied. Pairwise comparisons were made, with $P < 0.05$ indicating statistical significance. The experimental images were processed and analyzed using GraphPad Prism 9 software.

Results

Network pharmacology-based analysis of the interaction between Ejiao and key targets involved in COPD

Through network pharmacology and the collection of relevant literature,[25] 30 Ejiao compounds, 22 amino acids, and 35 trace elements were obtained. The main components of Ejiao and 30 Ejiao characteristic peptides are shown in Table 1 and File S1. By searching GeneCards, OMIM, and DrugBank, 2836 COPD-related targets and 703 Ejiao gelatin targets were identified, including 114 targets of Ejiao chemical components and 589 Ejiao polypeptide targets. Using Jvenn, a Venn diagram was generated, revealing 68 intersection targets (Fig. 1a). The intersection target data were imported into the STRING platform to obtain the protein-protein interaction network of Ejiao and COPD (Fig. 1b). The intersection genes were then entered into the DAVID database, and a total of 127 projects were obtained for GO enrichment analysis. Figure 1c shows the top 10 enriched terms in the categories of BP, CC, and MF. In the BP category, key processes include response to xenobiotic stimulus and negative regulation of cell population proliferation. The CC category encompasses structures such as plasma membrane, postsynaptic membrane, and neuron projection. The MF category includes functions such as nuclear receptor activity, signaling receptor binding, steroid binding, and heterocyclic compound binding. In the KEGG pathway enrichment analysis (Fig. 1d), the top 20 pathways identified were mainly concentrated in the calcium signaling and estrogen signaling pathways.

Ejiao protects against CSE-induced cell damage by regulating the ER pathway

Determine the optimal concentrations for CSE modeling and Ejiao-containing serum by assessing their effects on cell viability

The CCK8 method was used to assess cell viability. The results showed that Ejiao-containing serum had no significant effect on the growth of macrophages after 12 h of incubation (Fig. 2a). However, after 24 h of treatment, cell viability in all Ejiao-containing serum groups showed varying degrees of improvement (**$P < 0.01$, Fig. 2b). The inhibitory effect was more pronounced at 12 and 24 h after CSE treatment. When the CSE concentration was 20 µg/mL, cell viability decreased significantly at both 12 and 24 h of culture (**$P < 0.01$, Fig. 2c and d). Therefore, 10 µg/mL CSE was selected to stimulate RAW264.7 cells for 12 h, and the concentrations of the drug-containing serum group were selected at 5%, 10%, and 15% for subsequent experiments.

Ejiao improves CSE-induced inflammatory response and enhances the production of anti-inflammatory factors by activating the ER/AKT pathway

RAW264.7 cells were treated with CSE (10 µg/mL) for 12 h, followed by Western blot analysis to evaluate protein expression levels. The results demonstrated a significant increase in the inflammatory marker TNF-α in the model group compared to the control group (**$P < 0.01$). Notably, treatment with Ejiao at medium and high doses significantly reduced TNF-α levels in a dose-dependent manner compared to the model group. Concurrently, the anti-in-

Table 1. Main ingredients of Ejiao

	Element	CAS number	SMILES	Type
1	Dermatan sulfate	24967-94-0	CC(=O)NC1C(C(C(OC1O)CO)OS(=O)(=O)[O-])OC2C(C(C(C(O2)C(=O) [O-])O)O)O	Compound
2	Methane,isothiocyanato-9,12-Octadecadienoic	556-61-6	CN=C=S	Compound
3	Methyl octadeca-9,12-dienoate	2566-97-4	CCCCCC=CCC=CCCCCCCCC(=O)OC	Compound
4	Octadec-13-enal	58594-45-9	CCCCC=CCCCCCCCCCCCC=O	Compound
5	5-Methyl-6-heneicosen-11-one	NA	CCCCCCCCCCC(=O)CCCC=CC(C)CCCC	Compound
6	Cyclododecanone,2-Methylene-	3045-76-9	C=C1CCCCCCCCCCC1=O	Compound
7	Tetradecane,1-chloro-	2425-54-9	CCCCCCCCCCCCCCCl	Compound
8	Tetratriacontane	14167-59-0	CCCCCCCCCCCCCCCCCCCCCCCCCCCCCCCCCC	Compound
9	Heneicosane	629-94-7	CCCCCCCCCCCCCCCCCCCCC	Compound
10	Tricosane	638-67-5	CCCCCCCCCCCCCCCCCCCCCCC	Compound
11	Tetracosane	646-31-1	CCCCCCCCCCCCCCCCCCCCCCCC	Compound
12	Docosane, 1-bromo-	6938-66-5	CCCCCCCCCCCCCCCCCCCCCCBr	Compound
13	1-Iodononadecane	3386-33-2	CCCCCCCCCCCCCCCCCCCI	Compound
14	heptane,1-methyl-4-(2-methyloxiranyl)-	96-08-2	CC12CCC(CC1O2)C3(CO3)C	Compound
15	Oxacycloheptadecan-2-one	109-29-5	C1CCCCCCCC(=O)OCCCCCCC1	Compound
16	1,1-biphenyl, 3-(1- methylethyl)-2-Amino-6, 7-dimethyl-5,	20282-30-8	CC(C)C1=CC=CC(=C1)C2=CC=CC =C2	Compound
17	6, 7, 8-tetrahydro-4- pteridinol	611-54-12	CC1C(NC2=C(N1)C(=O)NC(=N2)N)C	Compound
18	Cyclohexene,4-(4-ethylcyclohexyl)-1-pentyl-	301643-32-3	CCCCCC1=CCC(CC1)C2CCC(CC2)CC	Compound
19	Aristolene epoxide	NA	CC1CCCC23C1(C4C(C4(C)C)CC2O3)C	Compound
20	p-Menth-8(10)-en-9-ol, cis-	5502-99-8	CC1CCC(CC1)C(=C)CO	Compound
21	13-Octadecenal,(Z)-	58594-45-9	CCCCC=CCCCCCCCCCCCC=O	Compound
22	8-Hexadecenal, 14- methyl-,(Z)-	60609-53-2	CCC(C)CCCCC=CCCCCCCC=O	Compound
23	Rhamnose	NA	C[C@H]1[C@@H]([C@H]([C@H](C(O1)O)O)O)O	Compound
24	Ethanol	64-17-5	CCO	Compound
25	p-Cresol	72269-62-6	CC1=CC=C(C=C1)O	Compound
26	Galactose	381716-33-2	C([C@@]1[C@@]([C@@]([C@](C(O1)O)O)O)O)O	Compound
27	2,1,3-Benzoxadiazol-4-amine, N-[(4-methoxyphenyl)methyl	488-17-5	NA	Compound
28	Glycerol	NA	C(C(CO)O)O	Compound
29	Maltose	NA	C([C@@H]1[C@H]([C@@H]([C@H]([C@H](O1)O[C@@H]2[C@H](O[C@H]([C@@H]([C@@H]([C@H]2O)O)O)CO)O)O)O)O)O	Compound
30	Sodium sulfate	NA	[O-]S(=O)(=O)[O-].[Na+].[Na+]	Compound
31	Aspartic acid	56-84-8	C(C(C(=O)O)N)C(=O)O	Amino acids
32	Threonine	72-19-5	CC(C(C(=O)O)N)O	Amino acids
33	Serine	56-45-1	C(C(C(=O)O)N)O	Amino acids
34	Glutamic acid	56-86-0	C(CC(=O)O)C(C(=O)O)N	Amino acids
35	Glycine	25718-94-9	C(C(=O)O)N	Amino acids
36	Alanine	56-41-7	CC(C(=O)O)N	Amino acids
37	Valine	72-18-4	CC(C)C(C(=O)O)N	Amino acids
38	Methionine	63-68-3	CSCCC(C(=O)O)N	Amino acids
39	Isoleucine	443-79-8	CCC(C)C(C(=O)O)N	Amino acids
40	Leucine	61-90-5	CC(C)CC(C(=O)O)N	Amino acids

(continued)

Table 1. *(continued)*

	Element	CAS number	SMILES	Type
41	Tyrosine	60-18-4	C1=CC(=CC=C1CC(C(=O)O)N)O	Amino acids
42	Phenylala	63-91-2	C1=CC=C(C=C1)CC(C(=O)O)N	Amino acids
43	Lysine	56-87-1	C(CCN)CC(C(=O)O)N	Amino acids
44	Cysteine	52-90-4	C(C(C(=O)O)N)S	Amino acids
45	Histidine	71-00-1	C1=C(NC=N1)CC(C(=O)O)N	Amino acids
46	Arginine	74-79-3	C(CC(C(=O)O)N)CN=C(N)N	Amino acids
47	Proline	4305-67-3	C1CC(NC1)C(=O)O	Amino acids
48	Tryptophane	73-22-3	C1=CC=C2C(=C1)C(=CN2)CC(C(=O)O)N	Amino acids
49	Hydroxyproline	618-28-0	C1C(CNC1C(=O)O)O	Amino acids
50	Decanoic acid	334-48-5	CCCCCCCCCC(=O)O	Amino acids
51	DL-Pyroglutamic acid	16891-48-8	C1CC(=O)NC1C(=O)O	Amino acids
52	L - Proline	NA	C1C[C@](NC1)C(=O)O	Amino acids
53	Iron sesquioxide	NA	NA	Trace elements
54	Calcium oxide	NA	NA	Trace elements
55	Magnesium oxide	NA	NA	Trace elements
56	Potassium oxide	NA	NA	Trace elements
57	Sodium oxide	NA	NA	Trace elements
58	Titanium dioxide	NA	NA	Trace elements
59	Manganese dioxide	NA	NA	Trace elements
60	Phosphorus pentoxide	NA	NA	Trace elements
61	Potassium	NA	NA	Trace elements
62	Sodium	NA	NA	Trace elements
63	Calcium	NA	NA	Trace elements
64	Magnesium	NA	NA	Trace elements
65	Iron	NA	NA	Trace elements
66	Copper	NA	NA	Trace elements
67	Aluminum	NA	NA	Trace elements
68	Manganese	NA	NA	Trace elements
69	Zinc	NA	NA	Trace elements
70	Chromium	NA	NA	Trace elements
71	Platinum	NA	NA	Trace elements
72	Stannum	NA	NA	Trace elements
73	Plumbum	NA	NA	Trace elements
74	Silver	NA	NA	Trace elements
75	Bromine	NA	NA	Trace elements
76	Molybdenum	NA	NA	Trace elements
77	Strontium	NA	NA	Trace elements
78	Barium	NA	NA	Trace elements
79	Cadmium	NA	NA	Trace elements
80	Cobalt	NA	NA	Trace elements
81	Niobium	NA	NA	Trace elements
82	Nickel	NA	NA	Trace elements
83	Strontium	NA	NA	Trace elements
84	Vanadium	NA	NA	Trace elements
85	Lanthanum	NA	NA	Trace elements
86	Thorium	NA	NA	Trace elements
87	Arsenic	7440-38-2	NA	Trace elements

CAS, Chemical Abstracts Service; NA, not available; SMILES, simplified molecular input line entry system.

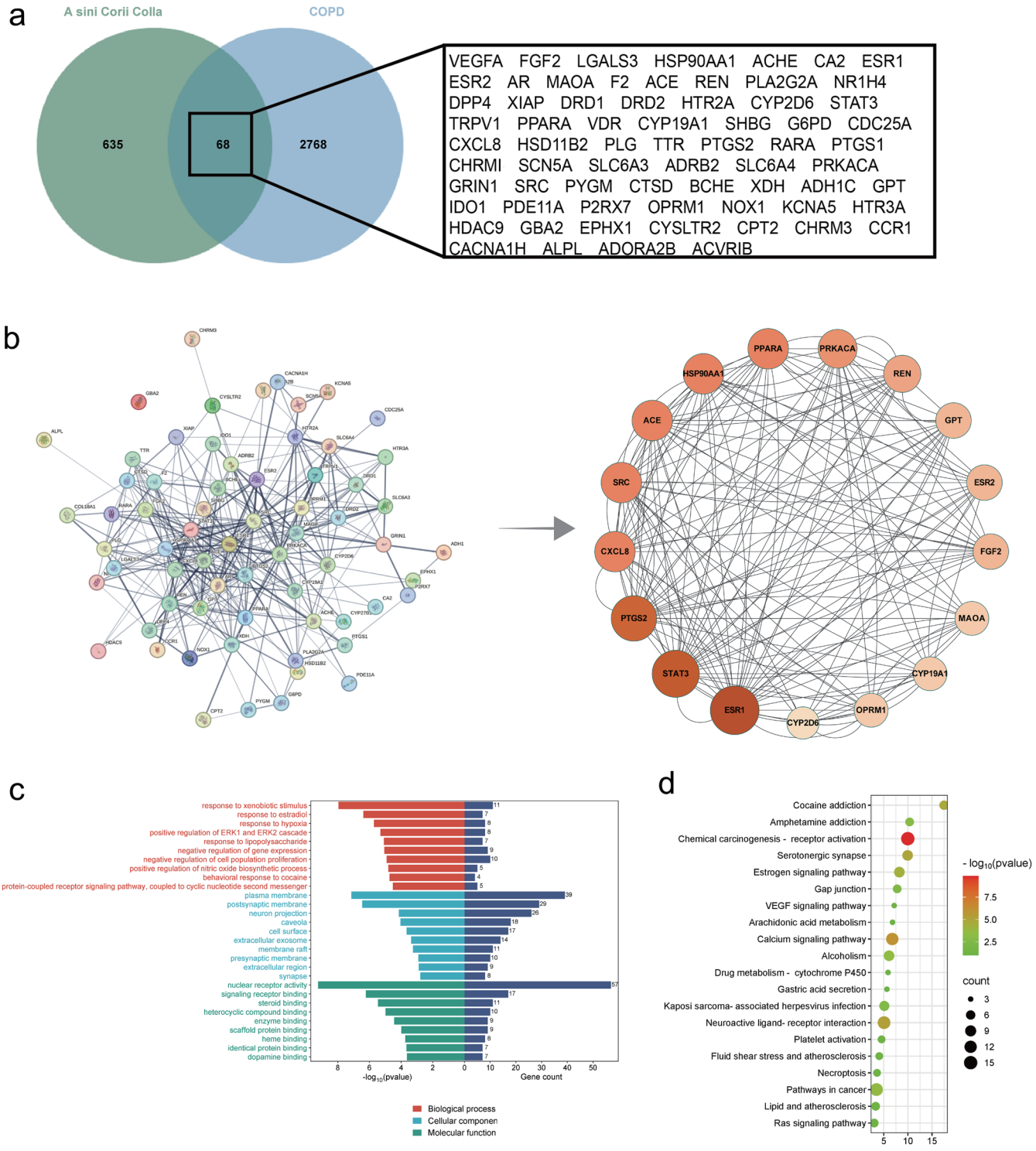

Fig. 1. Network pharmacology suggests the potential mechanism of Ejiao in regulating chronic obstructive pulmonary disease. (a, b) Construction and analysis of drug-disease targets; (c, d) GO and KEGG enrichment maps. GO, Gene Ontology; KEGG, Kyoto Encyclopedia of Genes and Genomes.

flammatory cytokine IL-10 was markedly upregulated in the medium- and high-dose Ejiao groups compared to the model group ($^{\#}P < 0.05$, $^{\#\#}P < 0.01$). Further analysis revealed that ERα+β expression levels were significantly decreased in the model group relative to the control group ($^{**}P < 0.01$), while phosphorylated AKT (p-AKT, Ser473) levels were significantly elevated ($^{**}P < 0.01$). High-dose Ejiao treatment restored ERα+β expression levels ($^{\#\#}P < 0.01$), suggesting that Ejiao may modulate estrogen receptor

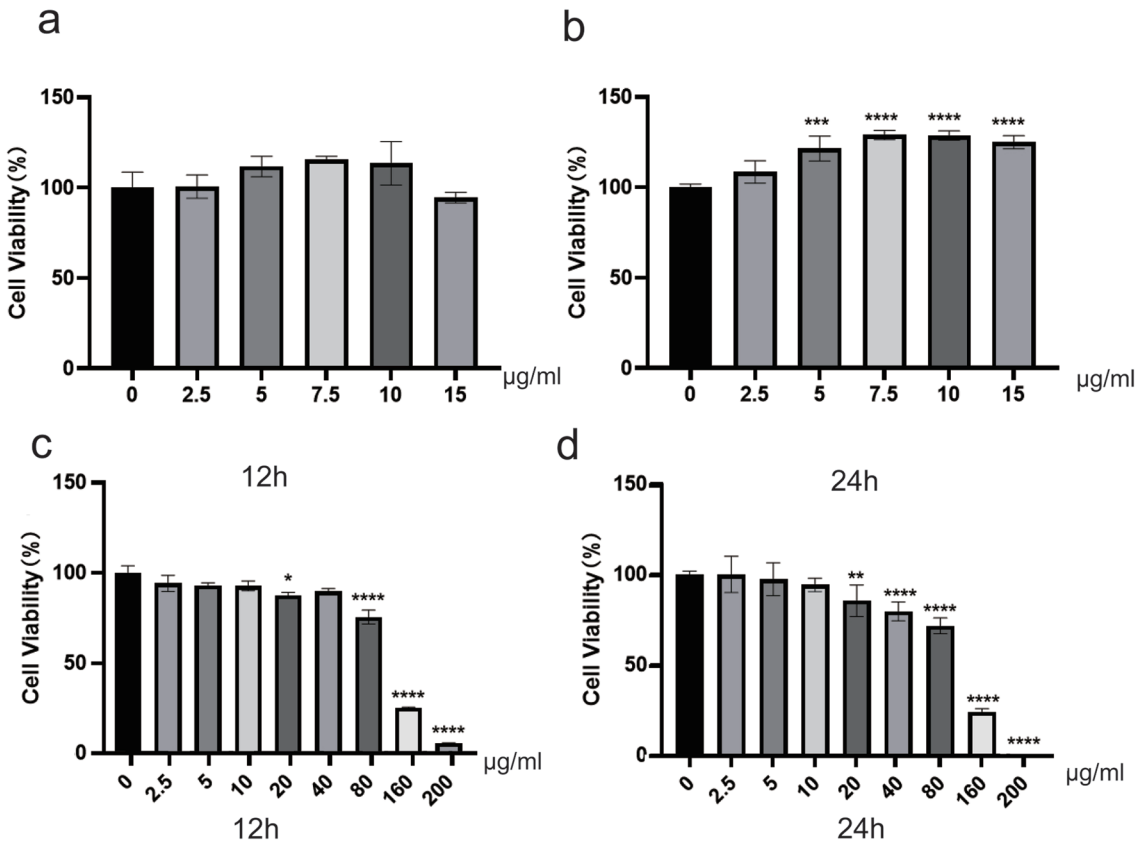

Fig. 2. CCK-8 cell viability test of RAW264.7 cells. (a) Effect of serum containing Ejiao on the suvival rate of RAW264.7 cells for 12 h; (b) Effect of serum containing Ejiao on the survival rate of RAW264.7 cells for 24 h; (c) Effect of CSE poisoning for 12 h on the suvival rate of RAW264.7 cells; (d) Effect of CSE poisoning for 24 h on the survival rate of RAW264.7 cells. Error bars represent SD ± mean of three independent experiments, n = 3, **P*<0.05, ***P*<0.01, ****P*<0.001, *****P*<0.0001. CCK-8, cell counting kit-8; CSE, cigarette smoke extract; SD, standard deviation.

expression and inhibit the AKT signaling pathway. Additionally, IκBα protein expression was significantly reduced in the model group compared to the control group (***P* < 0.01). This suggests that CSE treatment may activate the ER/AKT signaling pathway, influencing downstream inflammatory factor regulation. The findings indicate that Ejiao's protective effects may involve modulating the ER/AKT signaling pathway and restoring IκBα expression. The results are illustrated in Figure 3.

Ejiao alleviates CSE/LPS-induced COPD in mice via the ER/AKT/NF-κB pathway

The body weight of mice was monitored throughout the modeling period. Seven days after modeling, a weight reduction was observed across all groups, followed by gradual recovery. By the end of the experiment, there were no significant differences in body weight among the groups (Fig. 4a).

Ejiao improves lung function damage in COPD model mice in a dose-dependent manner

Lung function in the mice was assessed using the EMKA animal lung function detection system, with measurements recorded every two weeks to monitor changes over the course of the experiment. On day 42, compared to the control group, the lung function indicators in the model group showed that the expiratory interval time, inspiratory time, expiratory time, and mid-expiratory flow rate (EF50) were significantly reduced (**P* < 0.05), and the respiratory rate was significantly increased (****P* < 0.001), indicating that the model was successful. In terms of various lung function indicators, the Ejiao-treated groups showed significant improvement in lung function compared to the model group (Fig. 4b). In summary, the mice in the model group showed obvious lung function damage after modeling, and each medication group showed some improvement. On day 57, Flexivent forced oscillation lung function analysis revealed that, relative to the control group, the model group demonstrated elevated airway resistance (Rrs) and airway elastic resistance (Ers), decreased dynamic compliance of the respiratory system (Crs), worsened tissue damage (G), and reduced tissue elasticity (H) (**P* < 0.05). The model group showed significant decreases in IC, forced expiratory volume in 0.1 second (FEV0.1), 50% forced vital capacity (FVC), and Crs, and significant increases in G, H, Rrs, and Ers (**P* < 0.05). In contrast, the Ejiao administration group showed significant improvement across all lung function indicators, with the high-dose group showing statistically significant differences in IC, FEV0.1, 50% FVC, G, H, Crs, Rrs, and Ers compared to the model group ($^{\#\#}P < 0.01$). These effects were dose-dependent (Fig. 4c–k). The pressure-volume (PV)-Loops curve, detected by the SnapShot-150 module, reflected disease characteristics, with distinct morphological changes in the curves of different disease states (Fig. 4l). Evaluation of static compliance, deep inspiration volume, and slope revealed that, in contrast to the control group, the model group

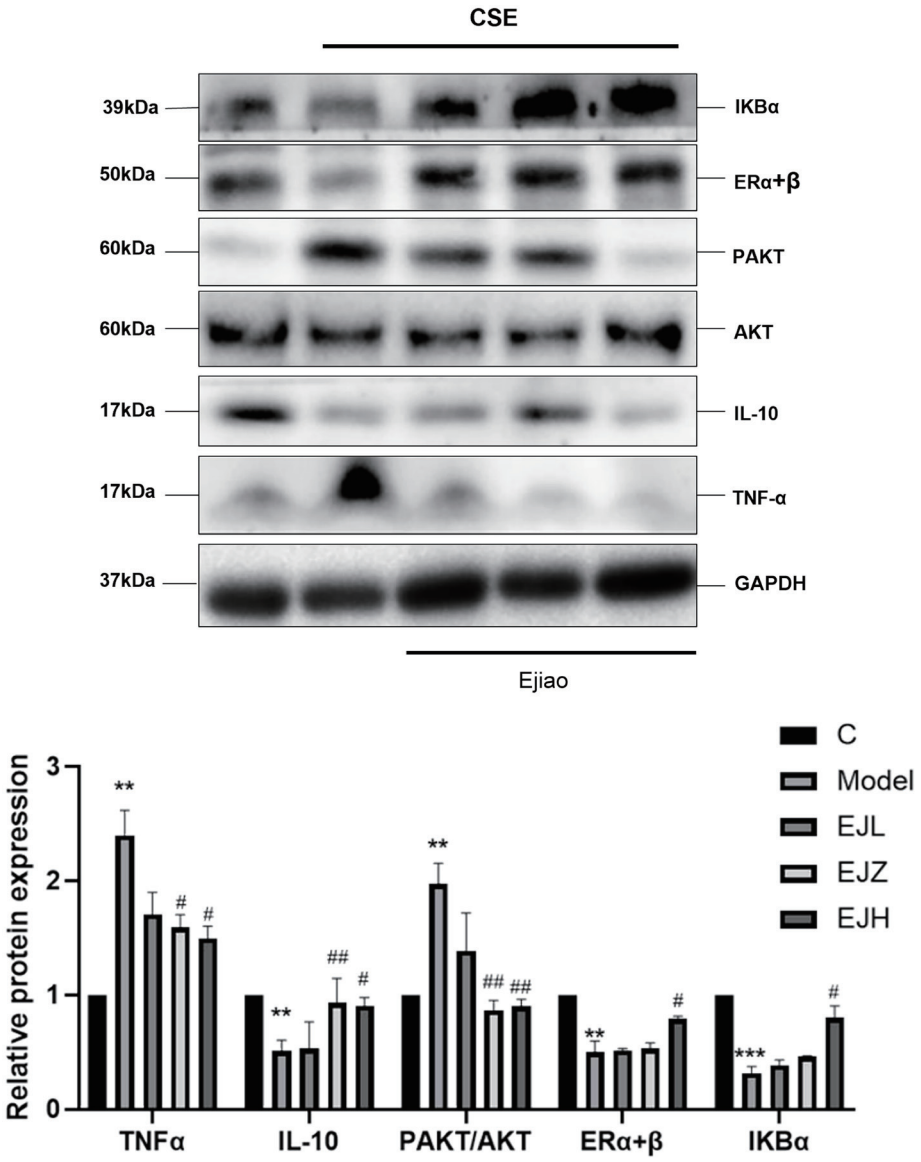

Fig. 3. Western blot was used to detect the expression of related proteins in CSE-infected RAW264.7 cells after treatment with Ejiao. Error bars represent SD ± mean values from three independent experiments, n = 3 per group. C is the Control group; M is the Model group; EJL is the Ejiao low dose group; EJZ is the Ejiao medium dose group; EJH is the Ejiao high dose group; Positive is the Roflumilast group. *$P < 0.05$, **$P < 0.01$, ***$P < 0.001$, model group compared with control group; $^{\#}P < 0.05$, $^{\#\#}P < 0.01$, drug administration group compared with model group. AKT, protein kinase B; CSE, cigarette smoke extract; ER, estrogen receptor; GAPDH, glyceraldehyde-3-phosphate dehydrogenase; IL, interleukin; PAKT, phosphorylated AKT; SD, standard deviation; TNFα, tumor necrosis factor alpha.

exhibited a downward shift in the PV loop, suggesting increased pressure requirements to achieve the target tidal volume, indicative of reduced compliance. Conversely, the PV loop for the Ejiao administration group was closer to the control group, with lower pressure requirements and better compliance. The dose-dependent improvement was clearly observed in the position of the PV-Loops curve (Fig. 4m–o).

Ejiao reduces peritoneal macrophage infiltration and improves inflammation and alveolar wall thickening in COPD mouse model

Flow cytometry analysis of mouse peritoneal macrophages (Fig. 5a–b) demonstrated that, relative to the solvent control group, the model group exhibited a marked elevation in the proportion of CD86+ CD11b+ F4/80+ macrophages (*$P < 0.05$). However, the content of CD86+ CD11b+ F4/80+ macrophages in the Ejiao group was reduced compared to the model group, with a significant difference observed in the high-dose Ejiao group ($^{\#\#}P < 0.01$).

Pathological histological analysis (Fig. 5c) showed that in the blank control and solvent control groups, there was no inflammatory cell infiltration around the bronchioles at any levels. Additionally, no bleeding or inflammatory cell exudation was observed in the alveolar cavity, and there was no obvious congestion in the alveolar wall. The alveolar walls maintained their normal thickness,

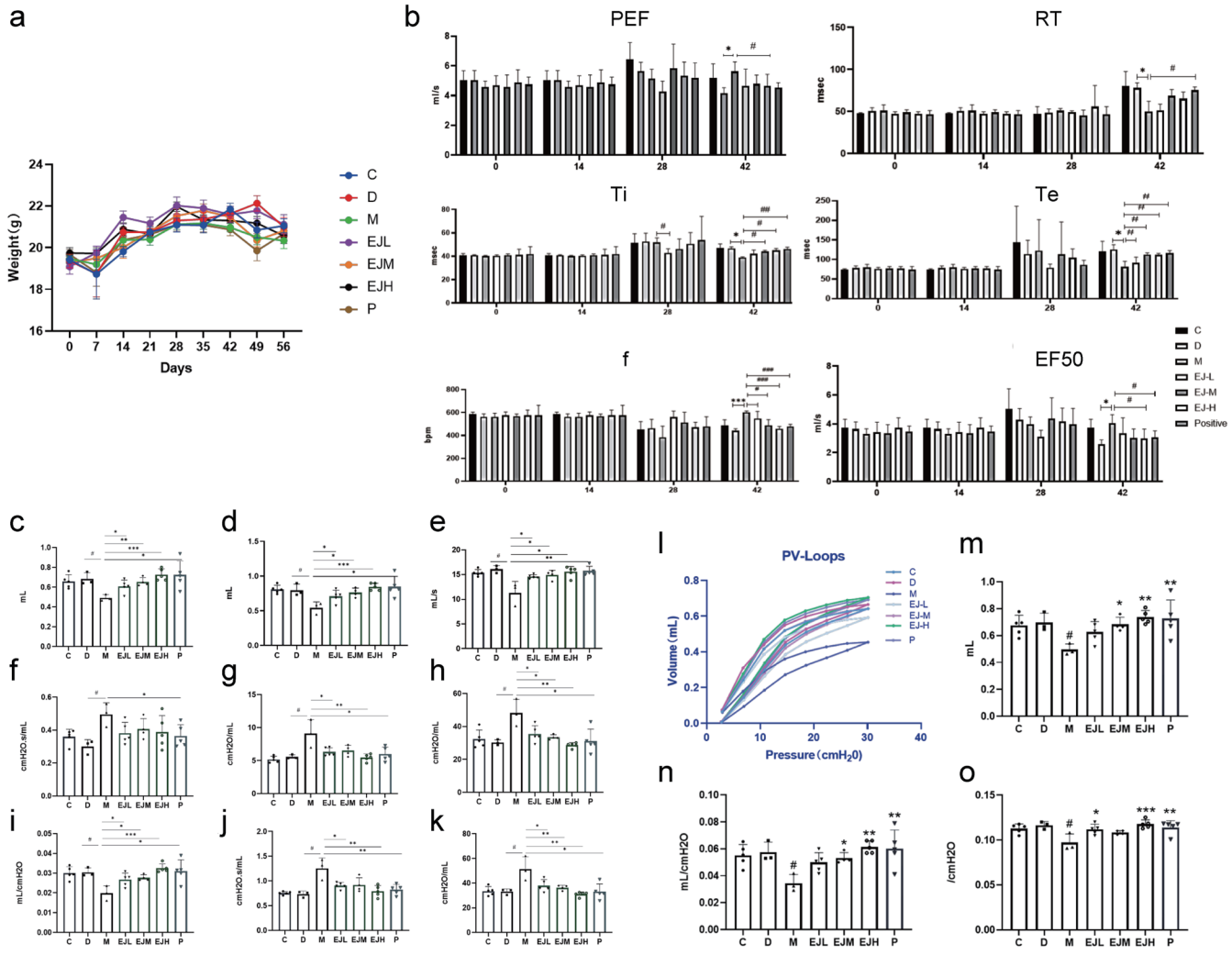

Fig. 4. Ejiao can improve lung function damage in COPD model mice. (a) Body weight data of drug-treated mice after nasal instillation of CSE combined with LPS induction. The weight of mice was recorded once a week to observe the rel ationship between weight changes in different groups; (b) After 42 days of CSE/LPS nasal drops and Ejiao treatment, EMKA was used to detect PEF, RT, Ti, f, Te, and EF50 to evaluate changes in lung function; FlexiVent forced oscillation small animal lung function test results (c-o): (c) inspiratory volume; (d) forced expiratory volume in the first 0.1s; (e) expiratory speed at 50% forced vital capacity; (f) central airway resistance; (g) tissue damage; (h) tissue flexibility; (i) total inspiratory resistance; (j) elastic resistance, (k) respiratory system compliance; (l) PV-Loops curve; (m) static compliance (Cst); (n) estimated value of deep inspiration volume (a); (o) slope of the curve (k). (C is Control group, D is DMSO group, M is Model group, EJL is EJiao low dose group, EJM is EJiao medium dose group, EJH is EJiao high dose group, P is Roflumilast group), **P*<0.05, ***P*<0.01, ****P*<0.001 model group compared with solvent group. $^{\#}P$<0.05, $^{\#\#}P$<0.01, $^{\#\#\#}P$<0.001 medication group compared with model group. COPD, chronic obstructive pulmonary disease; CSE, cigarette smoke extract; DMSO, dimethyl sulfoxide; EF50, expiratory flow at 50% of FVC; F, frequency; LPS, lipopolysaccharide; PEF, peak expiratory flow; PV, pressure-volume; RT, respiratory time; Te, expiratory time; Ti, inspiratory time.

and no transparent membrane formation was detected. In the model group, inflammatory cell exudation and infiltration around the alveolar cavity or vascular wall and alveolar wall thickening were observed. In the model group, animals showed exudation and infiltration of inflammatory cells around the alveolar cavity or vascular wall and alveolar wall thickening, with an average lesion score of 10.2, indicating that the model was successfully established. Congestion and hemorrhage, and/or exudation and infiltration of inflammatory cells around the alveolar cavity or vascular wall, and alveolar wall thickening were observed in the low-dose group, medium-dose group, high-dose group, and positive drug group, with average scores of 8.6, 6.4, 7.8, and 3, respectively. These results indicate that after treatment, the lesion scores were significantly reduced, suggesting that the administered drug had a beneficial effect in improving or alleviating the pathological changes.

Ejiao protects lung function by inhibiting inflammatory factors in lung tissue and estrogen levels in serum of COPD mice

ELISA was used to detect cytokines TNF-α, IL-1β, IL-10, and COX-2 in the BALF of mice. The results showed (Fig. 5d) that, compared with the solvent control, the levels of IL-1β, TNF-α, and COX-2 in the bronchoalveolar lavage fluid of the model group increased significantly, and the level of IL-10 decreased significantly (**P* < 0.05). Compared with the model group, the levels of IL-1β, TNF-α, and COX-2 in the bronchoalveolar lavage fluid of each administration group decreased significantly, and the level of IL-

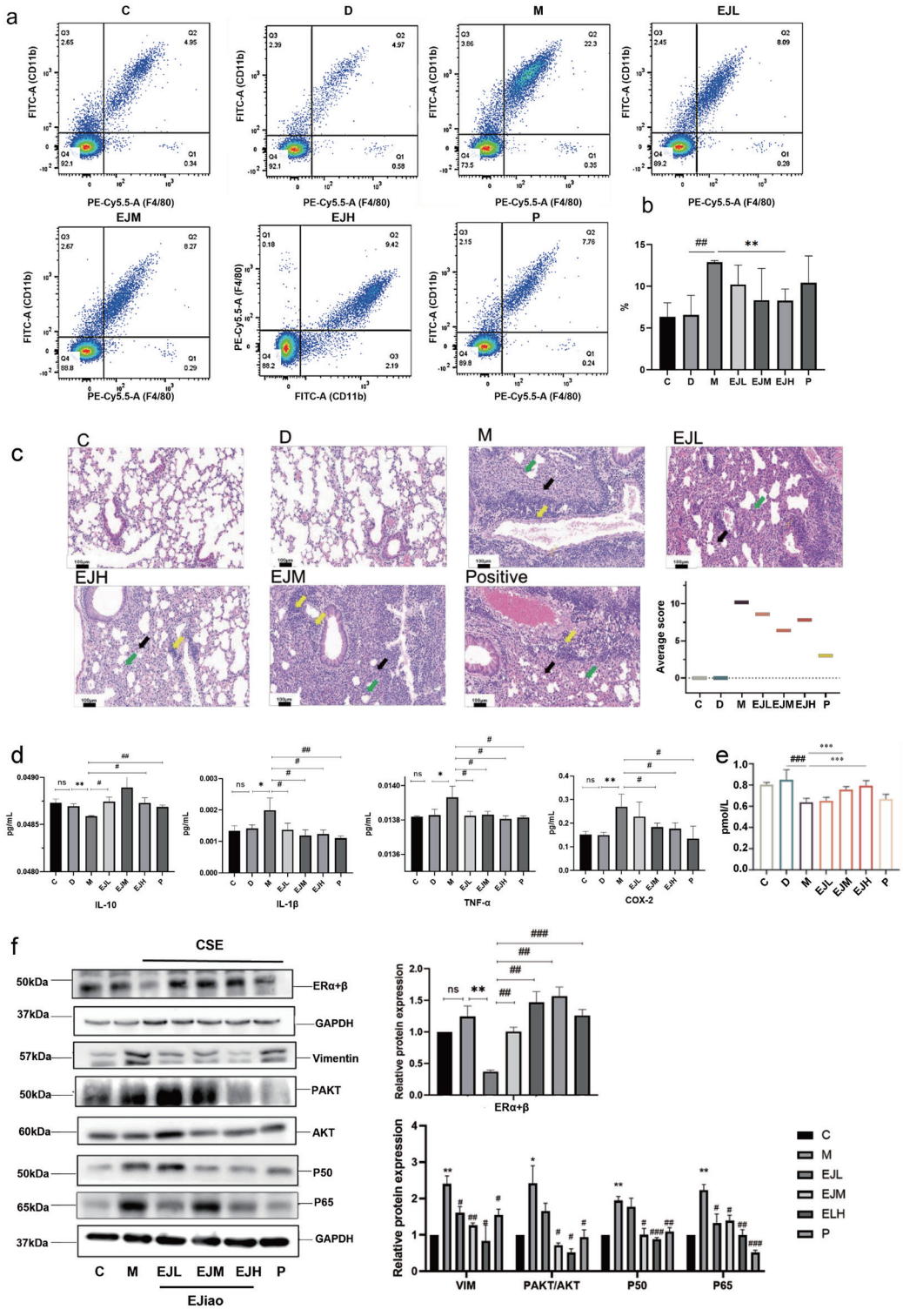

Fig. 5. Ejiao can reduce inflammatory factors in COPD mice. (a, b) Flow cytometry detection of CD86+ CD11b+ F4/80+macrophages in mouse peritoneal cavity, C is Control group; D is DMSO group; M is Model group; EJL is EJiao low dose group; EJM is EJiao medium dose group; EJH is EJiao high dose group; Positive is Roflumilast group; (c) Pictures and pathological scores of mouse lungs after modeling and treatment with Ejiao (inflammatory cell exudation is black arrow, infiltration is yellow arrow, and alveolar wall thickening is green arrow); (d) ELISA quantitative analysis of IL-10; IL-1β; TNF-α; COX-2 cytokine content in mouse bronchoalveolar lavage fluid; (e) E2 content in mouse serum; (f) ERα+β protein expression; Related pathways and inflammatory factor protein expression. **P*<0.05, ***P*<0.01, model group compared with control group; #*P*<0.05, ##*P*<0.01, ###*P*<0.001 drug-treated group compared with model group. COX-2, cyclooxygenase-2; DMSO, dimethyl sulfoxide; E2, estrogen; ELISA, enzyme-linked immunosorbent assay; ER, estrogen receptor; IL, interleukin; TNF-α, tumor necrosis factor alpha.

10 increased significantly ($^{\#}P < 0.05$, $^{\#\#}P < 0.01$). Additionally, serum estrogen levels were detected, revealing a significant increase in the Ejiao-treated groups compared to the model group, with a dose-dependent response. The Ejiao treatment groups showed a significant reduction in estrogen levels compared to the model group ($^{\#\#}P < 0.01$) (Fig. 5e).

Ejiao alleviates inflammatory response and cell proliferation/migration in COPD mice via the ER/AKT/NF-κB pathway

To further investigate the protective effects of Ejiao on CSE/LPS-induced COPD in mice, Western blot analysis was conducted to evaluate the protein levels associated with the ER/AKT/NF-κB signaling cascade, based on network pharmacology findings. The results showed that, compared with the solvent control group, the expression of ERα+β in the model group mice was significantly reduced ($^{**}P < 0.01$) (Fig. 5f), while the expression of p-AKT, Vimentin, NF-κB P50, and NF-κB P65 was significantly increased ($^{**}P < 0.01$) (Fig. 5g). These changes indicated that CSE/LPS induced an increase in inflammatory response and cell proliferation/migration, which was consistent with the characteristics of COPD. In contrast, compared with the model group, the expression of ERα+β in the Ejiao group was significantly increased ($^{\#\#}P< 0.01$) in a dose-dependent manner, and the expression of p-AKT, Vimentin, NF-κB P50, and NF-κB P65 was significantly decreased ($^{\#\#}P< 0.01$). These results suggest that Ejiao may enhance the expression of ERα+β and inhibit the activation of p-AKT, Vimentin, NF-κB P50, and NF-κB P65, thus alleviating the inflammatory response, cell proliferation, and migration, and providing protective effects in the COPD model.

Discussion

COPD is a progressive, irreversible inflammatory lung disorder that severely impairs respiratory function. Although there is no cure, treatments can manage symptoms and slow disease progression. COPD causes significant suffering, including persistent breathlessness, chronic cough, and fatigue, which severely affect daily life. Additionally, it imposes a substantial economic burden due to medical costs, frequent hospitalizations, and lost productivity. Ejiao, a traditional Chinese medicine known for its hematopoietic and blood-tonifying properties, has been shown to have therapeutic effects on lung function. Previous studies have demonstrated that Ejiao can improve lung function and reduce inflammation in COPD rat models.[26] Furthermore, in a rat lung injury model induced by intratracheal instillation of artificial PM2.5, Ejiao regulates disrupted metabolic pathways caused by artificial PM2.5 through the inhibition of Arg-1. This leads to a reduction in pulmonary inflammation, improvement in lung function, and protection against pathological lung damage.[20] Additionally, epidemiological studies have suggested that female reproductive factors may contribute to the development of COPD via hormonal influences, but experimental evidence supporting this hypothesis remains limited.[9] Existing studies have shown that most inflammatory proteins upregulated in COPD macrophages are regulated by the transcription factor NF-κB, which is activated in alveolar macrophages of COPD patients.[27] In *in vivo* models of COPD, exposure to cigarette smoke extract has been shown to increase NF-κB levels and its recruitment to the promoters of inflammatory genes in mouse lungs.[28] AKT can directly phosphorylate components of the IκB kinase complex, promoting the degradation of IκB and activating NF-κB.[29] In COPD lungs frequently exposed to cigarette smoke and airborne pathogens, the persistence of AKT-mediated inflammatory cell survival may be an integral process leading to the accumulation of macrophages, neutrophils, and T lymphocytes in the airways, parenchyma, and pulmonary vasculature. Macrophage and fibroblast proliferation in COPD aggravates inflammation and promotes airway fibrosis, leading to obstruction of small airways, and AKT can promote the proliferation of macrophages and fibroblasts in situ.[30] During acute exacerbations of COPD, AKT is involved in the upregulation of inflammatory protein expression, indicating that AKT not only supports chronic inflammation but also contributes significantly to the enhancement of the inflammatory response during exacerbations.[31] AKT plays a critical role in regulating inflammation and cell proliferation.[8] The interaction between ER and AKT signaling pathways mainly occurs during cell signaling. ER can be activated in both estrogen-dependent and independent manners, often involving signaling through PI3K and Akt, which have been shown to protect the heart from ischemic damage.[11] The results of this study align with these findings, suggesting that estrogen receptors may modulate NF-κB pathway activity by influencing upstream signaling molecules involved in this pathway. This regulatory effect may contribute to modulating the inflammatory responses and overall development of COPD.

Patients with chronic obstructive pulmonary disease often experience increased levels of oxidative stress, chronic inflammatory response, and immune suppression.[32] Currently, there are no specific treatments for COPD, and improving airflow limitation remains the main treatment goal. Most COPD treatment options involve inhaled drugs, including bronchodilators, inhaled corticosteroids, and other medications.[33] However, the side effects of these drugs cannot be ignored. For example, frequent use of inhaled corticosteroids may lead to osteoporosis, immunosuppression, and increased risk of infection, and may even promote the recurrence of COPD. Bronchodilators, especially anticholinergic drugs and β2 agonists commonly used in clinical practice, may cause side effects such as heart rate disorders, vision problems, urinary retention, and metabolic disorders.[34] In light of these concerns, this study investigates the potential of Ejiao as an adjunctive therapy for COPD. By combining database analysis with *in vitro* and *in vivo* experiments, we aimed to elucidate the mechanisms by which Ejiao may improve COPD outcomes. This research provides valuable theoretical support for the use of Ejiao in clinical COPD management, with the potential to enhance patient survival rates while promoting the modernization of traditional Chinese medicine. Through this approach, Ejiao may offer a safer alternative or complementary treatment strategy for COPD, addressing both the inflammatory and immune aspects of the disease. In conclusion, this study demonstrates that Ejiao exhibits significant therapeutic potential in alleviating lung injury and inflammatory responses associated with COPD. Through network pharmacology analysis, we identified that Ejiao may exert its pharmacological effects by modulating the estrogen receptor signaling pathway, a finding that was further verified by *in vitro* and *in vivo* experiments. The experimental results showed that Ejiao intervention significantly upregulated the expression levels of anti-inflammatory markers, including IL-10, ERα+β, and IκBα, while effectively suppressing the expression of pro-inflammatory markers, such as p-AKT and TNF-α. In the COPD mouse model, Ejiao treatment not only significantly improved lung function parameters but also reduced pulmonary macrophage infiltration and regulated the levels of inflammatory cytokines in BALF. For the first time, we investigated the potential regulatory effects of Ejiao on COPD via the ER/AKT/NF-κB pathway. With ongoing research, the therapeutic potential of

natural medicines in COPD treatment is becoming increasingly evident, particularly in symptom relief and disease progression delay, highlighting their potential as important adjunct therapies.

However, certain limitations exist in the design of this study. For instance, we evaluated the efficacy of Ejiao in COPD using a single-sex animal model, without fully considering potential sex differences. Given that our findings suggest Ejiao may regulate COPD progression via the estrogen receptor, future studies should focus on validating this mechanism in female mice. Additionally, although we initially explored the main active components of Ejiao through network pharmacology, we have not yet conducted an in-depth analysis of its key monomeric compounds in liver fibrosis, instead treating Ejiao as a whole. This holistic approach aligns with the traditional characteristics of Chinese medicine, where therapeutic effects are often achieved through the synergy of multiple components. However, with advancements in modern analytical techniques such as mass spectrometry, the identification and validation of active targets in natural medicines have become increasingly important, not only for elucidating their mechanisms of action but also for minimizing adverse drug reactions. Therefore, future studies will focus on identifying and validating the key active components of Ejiao responsible for lung function protection, thereby advancing its precise therapeutic application.

Conclusions

Ejiao can significantly improve the lung function indicators of COPD model mice, reduce the content of inflammatory factors in bronchoalveolar lavage fluid, increase the estrogen content in serum, and reduce the number of peritoneal macrophages. HE pathological observation and Western blot analysis showed that Ejiao can improve lung injury, and its mechanism of action may involve regulating estrogen levels in the body and affecting the ER/AKT/NF-κB signaling pathway, thereby alleviating inflammatory response and improving lung injury.

Acknowledgments

None.

Funding

This study was supported by the National Natural Science Foundation of China (82074104) and the National Natural Science Foundation of China (8247143489).

Conflict of interest

Bin Wang and Hongtao Jin serve as editorial board members of *Future Integrative Medicine*. Hongtao Jin, Wanfang Li and Xiangfeng Ye are employed by the company Beijing Union-Genius Pharmaceutical Technology Development Co. Ltd. The authors have no other conflicts of interest related to this publication.

Author contributions

Study concept and design (SS, TZ, XF), acquisition of data (TZ, HJ), analysis and interpretation of data (SS, JL, ZX), drafting of the manuscript (SS, TZ), critical revision of the manuscript for important intellectual content (WL, XY, CW), administrative, technical, or material support (PS, FX, HJ), and study supervision (BW, HJ). All authors have made significant contributions to this study and have approved the final manuscript.

Ethical statement

The experimental protocol applied in this study was approved by the Ethics Committee for Animal Experimentation of the New Drug Safety Evaluation Center, Institute of Materia Medica, Chinese Academy of Medical Sciences and Peking Union Medical College (ID: PDE-2301). All procedures complied with the Animal Research: Reporting of *In Vivo* Experiments guidelines and were performed according to the guidelines of the National Institutes for Animal Research. All researchers in this study were certified by the Animal Experimentation Center of the New Drug Safety Evaluation Center, Institute of Materia Medica, Chinese Academy of Medical Sciences and Peking Union Medical College.

Data sharing statement

The data used to support the findings of this study are available from the corresponding author upon reasonable request.

References

[1] Upadhyay P, Wu CW, Pham A, Zeki AA, Royer CM, Kodavanti UP, *et al*. Animal models and mechanisms of tobacco smoke-induced chronic obstructive pulmonary disease (COPD). J Toxicol Environ Health B Crit Rev 2023;26(5):275–305. doi:10.1080/10937404.2023.2208886, PMID:37183431.

[2] Uwagboe I, Adcock IM, Lo Bello F, Caramori G, Mumby S. New drugs under development for COPD. Minerva Med 2022;113(3):471–496. doi:10.23736/S0026-4806.22.08024-7, PMID:35142480.

[3] Liu D, Xu W, Tang Y, Cao J, Chen R, Wu D, *et al*. Nebulization of risedronate alleviates airway obstruction and inflammation of chronic obstructive pulmonary diseases via suppressing prenylation-dependent RAS/ERK/NF-κB and RhoA/ROCK1/MLCP signaling. Respir Res 2022;23(1):380. doi:10.1186/s12931-022-02274-5, PMID:36575527.

[4] Saito T, Fujino N, Kyogoku Y, Yamada M, Okutomo K, Ono Y, *et al*. Identification of Siglec-1-negative alveolar macrophages with proinflammatory phenotypes in chronic obstructive pulmonary disease. Am J Physiol Lung Cell Mol Physiol 2024;326(6):L672–L686. doi:10.1152/ajplung.00303.2023, PMID:38530936.

[5] Chakinala RC, Khatri A, Gupta K, Koike K, Epelbaum O. Sphingolipids in COPD. Eur Respir Rev 2019;28(154):190047. doi:10.1183/16000617.0047-2019, PMID:31694841.

[6] Zhao Z, Tong Y, Kang Y, Qiu Z, Li Q, Xu C, *et al*. Sodium butyrate (SB) ameliorated inflammation of COPD induced by cigarette smoke through activating the GPR43 to inhibit NF-κB/MAPKs signaling pathways. Mol Immunol 2023;163:224–234. doi:10.1016/j.molimm.2023.10.007, PMID:37864932.

[7] Liu Y, Kong H, Cai H, Chen G, Chen H, Ruan W. Progression of the PI3K/Akt signaling pathway in chronic obstructive pulmonary disease. Front Pharmacol 2023;14:1238782. doi:10.3389/fphar.2023.1238782, PMID:37799975.

[8] Guo Q, Jin Y, Chen X, Ye X, Shen X, Lin M, *et al*. NF-κB in biology and targeted therapy: new insights and translational implications. Signal Transduct Target Ther 2024;9(1):53. doi:10.1038/s41392-024-01757-9, PMID:38433280.

[9] Liang C, Chung HF, Dobson A, Sandin S, Weiderpass E, Mishra GD. Female reproductive histories and the risk of chronic obstructive pulmonary disease. Thorax 2024;79(6):508–514. doi:10.1136/thorax-2023-220388, PMID:38350732.

[10] Xia W, Pan Z, Zhang H, Zhou Q, Liu Y. ERRα protects against sepsis-induced acute lung injury in rats. Mol Med 2023;29(1):76. doi:10.1186/s10020-023-00670-1, PMID:37340376.

[11] Lou Y, Fu Z, Tian Y, Hu M, Wang Q, Zhou Y, *et al*. Estrogen-sensitive activation of SGK1 induces M2 macrophages with anti-inflammatory

properties and a Th2 response at the maternal-fetal interface. Reprod Biol Endocrinol 2023;21(1):50. doi:10.1186/s12958-023-01102-9, PMID:37226177.
[12] Chen P, Li B, Ou-Yang L. Role of estrogen receptors in health and disease. Front Endocrinol (Lausanne) 2022;13:839005. doi:10.3389/fendo.2022.839005, PMID:36060947.
[13] Browne IM, André F, Chandarlapaty S, Carey LA, Turner NC. Optimal targeting of PI3K-AKT and mTOR in advanced oestrogen receptor-positive breast cancer. Lancet Oncol 2024;25(4):e139–e151. doi:10.1016/S1470-2045(23)00676-9, PMID:38547898.
[14] Li Z, Chen BF, Huang JM, Huang JK, Huang Q, TAN JB. Effects of gelatina nigra on cytoimmunity and humoral immunity function in mice. Chin J Health Lab Technol 2008;18(7):1426-1427+1437.
[15] You Y, Wang K, Miao M, Zhang Y, Yuan H. Application of Ejiao(Asini Corii Colla) in Shennong's Classic of Materia Medica and Classic Formulas. Journal of Shandong University of Traditional Chinese Medicine 2024;48(6):679–684. doi:10.16294/j.cnki.1007-659x.2024.06.007.
[16] Qu YX, Fu YJ. Advances in Chemical Constituents, Quality Control and Pharmacological Effects of Asini corii colla. Special Wild Economic Animal and Plant Research 2023;45(3):136–143. doi:10.16720/j.cnki.tcyj.2023.090.
[17] Zhao FD, Dong JC, Cui Y, Xie JY, Wu SM. The Effect of Ejiao on Airway Inflammation and Th1/Th2 Cytokines in Serum of Asthmatic Rats. Chin J Exp Tradit Med Formulae 2006;12(6):59–61. doi:10.13422/j.cnki.syfjx.2006.06.022.
[18] Yue Q, Zhang W, Lin S, Zheng T, Hou Y, Zhang Y, *et al*. Ejiao ameliorates lipopolysaccharide-induced pulmonary inflammation via inhibition of NFκB regulating NLRP3 inflammasome and mitochondrial ROS. Biomed Pharmacother 2022;152:113275. doi:10.1016/j.biopha.2022.113275, PMID:35714510.
[19] Zhang PP, Ling YH, Yan XD, Wei JF, Jin HT, Wang AP. Protective effects of Colla Corii Asini on artificial fine particulate matter-induced respiratory system injury in rats. Carcinogenesis, Teratogenesis & Mutagenesis 2017;29(5):346–351. doi:10.3969/j.issn.1004-616x.2017.05.005.
[20] Liu T, Zhang P, Ling Y, Hu G, Gu J, Yang H, *et al*. Protective Effect of Colla corii asini against Lung Injuries Induced by Intratracheal Instillation of Artificial Fine Particles in Rats. Int J Mol Sci 2018;20(1):55. doi:10.3390/ijms20010055, PMID:30583600.
[21] Lugg ST, Scott A, Parekh D, Naidu B, Thickett DR. Cigarette smoke exposure and alveolar macrophages: mechanisms for lung disease. Thorax 2022;77(1):94–101. doi:10.1136/thoraxjnl-2020-216296, PMID:33986144.
[22] Han J, Hou J, Liu Y, Liu P, Zhao T, Wang X. Using Network Pharmacology to Explore the Mechanism of Panax notoginseng in the Treatment of Myocardial Fibrosis. J Diabetes Res 2022;2022:8895950. doi:10.1155/2022/8895950, PMID:35372585.
[23] Zhang Y, Li Z, Wei J, Kong L, Song M, Zhang Y, *et al*. Network pharmacology and molecular docking reveal the mechanism of Angelica dahurica against Osteosarcoma. Medicine (Baltimore) 2022;101(44):e31055. doi:10.1097/MD.0000000000031055, PMID:36343039.
[24] Wang C, Liu X, Guo S. Network pharmacology-based strategy to investigate the effect and mechanism of α-solanine against glioma. BMC Complement Med Ther 2023;23(1):371. doi:10.1186/s12906-023-04215-1, PMID:37865727.
[25] Wang D, Ru W, Xu Y, Zhang J, He X, Fan G, *et al*. Chemical constituents and bioactivities of Colla corii asini. Drug Discov Ther 2014;8(5):201–207. doi:10.5582/ddt.2014.01038, PMID:25382554.
[26] Nazakaiti·Ainiwar, Hu G, Zhang TT, Song MY, Zhao HM, Jin HT, *et al*. Effects of Colla corii asini on lung function and pathological injury in rats with chronic obstructive pulmonary disease. Basic & Clinical Medicine 2021;41(7):970–974. doi:10.16352/j.issn.1001-6325.2021.07.004.
[27] Barnes PJ. Inflammatory mechanisms in patients with chronic obstructive pulmonary disease. J Allergy Clin Immunol 2016;138(1):16–27. doi:10.1016/j.jaci.2016.05.011, PMID:27373322.
[28] Chen J, Wang T, Li X, Gao L, Wang K, Cheng M, *et al*. DNA of neutrophil extracellular traps promote NF-κB-dependent autoimmunity via cGAS/TLR9 in chronic obstructive pulmonary disease. Signal Transduct Target Ther 2024;9(1):163. doi:10.1038/s41392-024-01881-6, PMID:38880789.
[29] Hussain AR, Ahmed SO, Ahmed M, Khan OS, Al Abdulmohsen S, Platanias LC, *et al*. Cross-talk between NFkB and the PI3-kinase/AKT pathway can be targeted in primary effusion lymphoma (PEL) cell lines for efficient apoptosis. PLoS One 2012;7(6):e39945. doi:10.1371/journal.pone.0039945, PMID:22768179.
[30] Bozinovski S, Vlahos R, Hansen M, Liu K, Anderson GP. Akt in the pathogenesis of COPD. Int J Chron Obstruct Pulmon Dis 2006;1(1):31–38. doi:10.2147/copd.2006.1.1.31, PMID:18046900.
[31] Wang C, Zhou J, Wang J, Li S, Fukunaga A, Yodoi J, *et al*. Progress in the mechanism and targeted drug therapy for COPD. Signal Transduct Target Ther 2020;5(1):248. doi:10.1038/s41392-020-00345-x, PMID:33110061.
[32] Li D, Xue XM, Cai HY, Zhang Y, Meng LH, Qiao WX, *et al*. Study on the mechanism of autophagy-related genes in the treatment of chronic obstructive pulmonary disease with Xuanfei Pingchuan capsule based on transcriptome sequencing. Lishizhen Medicine and Materia Medica Research 2024;35(12):2891–2897. doi:10.3969/j.issn.1008-0805.2024.12.33.
[33] Chinese Medical Association, Chinese Medical Association Publishing House, Chinese Society of General Practice, Chronic Obstructive Pulmonary Disease Study Group of Chinese Thoracic Society, Editorial Board of Chinese Journal of General Practitioners of Chinese Medical Association, Expert Group of Guidelines for Primary Care of Respiratory System Disease, *et al*. Chinese guideline for management of chronic obstructive pulmonary disease in primary care (2024). Chinese . Journal of General Practice 2024;23(6):578–602. doi:10.3760/cma.j.cn114798-20240326-00174.
[34] Guo P, Li R, Piao TH, Wang CL, Wu XL, Cai HY. Pathological Mechanism and Targeted Drugs of COPD. Int J Chron Obstruct Pulmon Dis 2022;17:1565–1575. doi:10.2147/COPD.S366126, PMID:35855746.